ELECTRON DENSITY DIAGNOSTICS FOR GASEOUS NEBULAE INVOLVING THE O IV INTERCOMBINATION LINES NEAR 1400 Å

F. P. KEENAN, E. S. CONLON, AND D. A. BOWDEN

Department of Pure and Applied Physics, The Queen's University of Belfast,

Belfast BT7 1NN, Northern Ireland, UK

W. A. FEIBELMAN[1]

Laboratory for Astronomy and Solar Physics, Code 684.1, NASA–Goddard

Space Flight Center, Greenbelt MD 20771

AND

A. K. PRADHAN

Department of Astronomy, The Ohio State University, Columbus OH 43210

ABSTRACT

Theoretical O IV electron density sensitive emission line ratios, determined using electron impact excitation rates calculated with the R-matrix code, are presented for $R_1 = I(1407.4 \text{ Å})/I(1401.2 \text{ Å})$, $R_2 = I(1404.8 \text{ Å})/I(1401.2 \text{ Å})$, $R_3 = I(1399.8 \text{ Å})/I(1401.2 \text{ Å})$ and $R_4 = I(1397.2 \text{ Å})/I(1401.2 \text{ Å})$. The observed values of $R_1 - R_4$, measured from high resolution spectra obtained with the *International Ultraviolet Explorer* (IUE) satellite, lead to electron densities that are compatible, and which are also in good agreement with those deduced from line ratios in other species. This provides observational support for the accuracy of the atomic data adopted in the present calculations.

Subject headings: atomic data — binaries: symbiotic — planetary nebulae: general — ultraviolet: stars

2
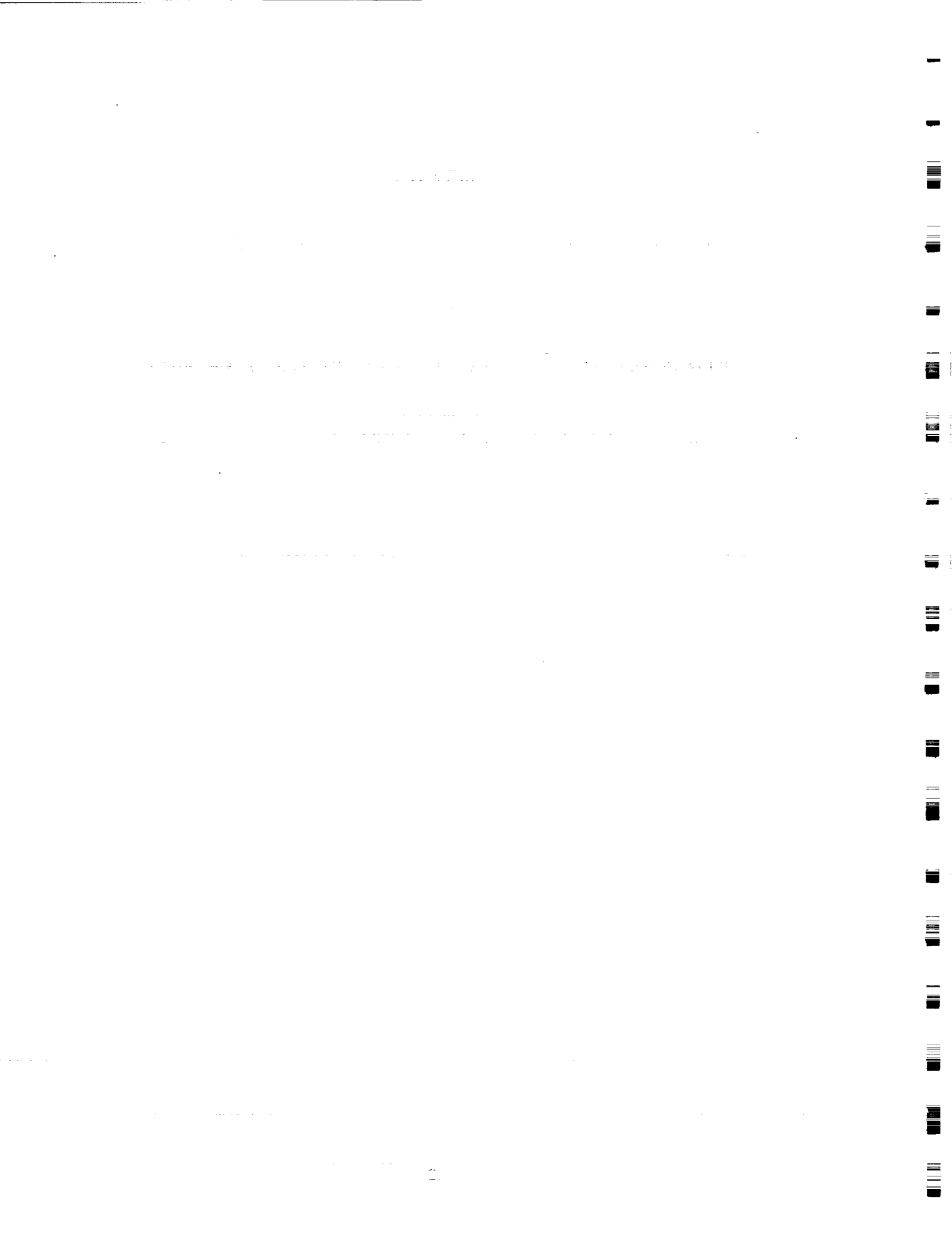
1. INTRODUCTION

The O IV $2s^2 2p$ ^{2}P $-$ $2s2p^2$ ^{4}P intercombination lines near 1400 Å have been observed in the spectra of astrophysical sources, including planetary nebulae (Hayes & Nussbaumer 1983), symbiotic stars (Feibelman 1982), and the solar transition region (Sandlin et al. 1986). Flower & Nussbaumer (1975) first pointed out the diagnostic applications of emission line ratios involving these transitions, and presented relative line strengths determined using electron impact excitation rates calculated in the distorted-wave approximation (Eissner & Seaton 1972). Hayes & Nussbaumer (1983) subsequently rederived these ratios using more accurate electron rates deduced with the IMPACT computer code of Crees, Seaton, & Wilson (1978).

Recently Blum & Pradhan (1992) have calculated excitation rates for transitions in O IV using the R-matrix method as adapted for the Opacity Project (Seaton 1987; Berrington et al. 1987), and found results somewhat different from those of Hayes & Nussbaumer (1983). For example, at $T_e = 5000$ K, the Blum & Pradhan rate for the $2s^2 2p$ ^{2}P$_{1/2}$ $-$ $2s2p^2$ ^{4}P$_{1/2}$ transition is $\sim$15% larger than that of Hayes & Nussbaumer, while for the $2s2p^2$ ^{4}P$_{1/2}$ $-$ $2s2p^2$ ^{4}P$_{5/2}$ transition the R-matrix data are $\sim$20% larger. In this paper we use the Blum & Pradhan results to derive emission line ratios applicable to gaseous nebulae, and compare these with observations obtained with the *International Ultraviolet Explorer* (IUE) satellite.

2. THEORETICAL RATIOS

The model ion for O IV consisted of the 15 energetically lowest fine-structure levels, namely $2s^2 2p$ $^2P_{1/2,3/2}$; $2s2p^2$ $^4P_{1/2,3/2,5/2}$, $^2D_{3/2,5/2}$, $^2S_{1/2}$, $^2P_{1/2,3/2}$; $2p^3$ $^4S_{3/2}$, $^2D_{3/2,5/2}$ and $^2P_{1/2,3/2}$. Energies for all these levels were obtained from Fawcett (1975).

Electron impact excitation rates for transitions in O IV were taken from Blum & Pradhan (1992), while for Einstein A-coefficients the calculations of Nussbaumer & Storey (1982) and Dankworth & Trefftz (1977) were adopted. As noted by, for example Seaton (1964), excitation by protons may be important for fine-structure transitions. However Flower & Nussbaumer (1975) found proton rates for transitions within $2s^2 2p$ ^2P and $2s2p^2$ ^4P to be typically a factor of 100 smaller than the corresponding electron rates at the temperatures considered here. Hence these rates should have a negligible effect on the theoretical line intensities for O IV.

Using the atomic data discussed above in conjunction with the statistical equilibrium code of Dufton (1977), relative O IV level populations and hence emission line strengths were calculated for a range of electron temperatures and densities. The following assumptions were made in the calculations, (i) that photoexcitation and de-excitation rates are negligible in comparison with the corresponding collisional rates, (ii) that ionization to and recombination from other ionic levels is slow compared with bound-bound rates, and (iii) that all transitions are optically thin. Further details of the procedures involved may be found in Dufton (1977) and Dufton et al. (1978).

In Figures 1 and 2 we plot the theoretical ratios

$$R_1 = I(2s^2 2p \ ^2P_{3/2} - 2s2p^2 \ ^4P_{1/2})/I(2s^2 2p \ ^2P_{3/2} - 2s2p^2 \ ^4P_{5/2})$$

$$= I(1407.4 \text{ Å})/I(1401.2 \text{ Å}),$$

$$R_2 = I(2s^22p\ ^2P_{3/2} - 2s2p^2\ ^4P_{3/2})/I(2s^22p\ ^2P_{3/2} - 2s2p^2\ ^4P_{5/2})$$

$$= I(1404.8 \text{ Å})/I(1401.2 \text{ Å})$$

as a function of electron density for a range of electron temperatures, $T_e = 5000 - 40000$ K. An inspection of the figures reveals that the temperature dependence of the ratios is small, but that they vary with density for $N_e \geq 10^2$ cm^{-3}. For example, at $T_e = 10000$ K, R_1 and R_2 change by factors of 2.8 and 2.1, respectively, between $N_e = 10^2$ and 10^6 cm^{-3}. However the variation in the ratios between $T_e = 10000$ and 20000 K is only 11% (R_1) and 9% (R_2) at $N_e = 10^2$ cm^{-3}, which decreases to 2% (R_1) and 1% (R_2) at $N_e = 10^6$ cm^{-3}. We note that the ratios

$$R_3 = I(2s^22p\ ^2P_{1/2} - 2s2p^2\ ^4P_{1/2})/I(2s^22p\ ^2P_{3/2} - 2s2p^2\ ^4P_{5/2})$$

$$= I(1399.8 \text{ Å})/I(1401.2 \text{ Å}),$$

$$R_4 = I(2s^22p\ ^2P_{1/2} - 2s2p^2\ ^4P_{3/2})/I(2s^22p\ ^2P_{3/2} - 2s2p^2\ ^4P_{5/2})$$

$$= I(1397.2 \text{ Å})/I(1401.2 \text{ Å})$$

have the same density dependence due to common upper levels as R_1 and R_2, respectively, but with

$$R_3 = 0.987 \times R_1,$$

$$R_4 = 0.176 \times R_2.$$

The present calculations in Figures 1 and 2 may be compared with those of Hayes & Nussbaumer (1983). Our results for R_1 and R_2 are up to $\sim$15%

different from those of Hayes & Nussbaumer, which is principally due to the adoption of improved electron impact excitation rates in the present analysis.

3. RESULTS AND DISCUSSION

Observed values of R_1 – R_4 have been measured from high resolution ul-traviolet spectra obtained with the IUE satellite. The objects considered (the planetary nebulae NGC 3918 and NGC 7662, and the symbiotic stars RR Tel and V1016 Cyg) are listed in Table 1, along with the IUE images used in the analysis. Also given are the derived emission line ratios, which were deter-mined using the Goddard Regional Data Reduction Facility. We note that the O IV 1404.8 Å feature is blended with the S IV $3s^23p$ $^2P_{1/2}$ – $3s3p^2$ $^4P_{1/2}$ line. However this S IV transition is predicted to be $\leq 20\%$ of the intensity of the S IV $3s^23p$ $^2P_{3/2}$ – $3s3p^2$ $^4P_{5/2}$ component at 1406.0 Å (Dufton et al. 1982). From the extreme weakness (or absence) of the 1406.0 Å line in our spectra, we estimate that S IV contributes $\leq 3\%$ to the total strength of the O IV/S IV 1404.8 Å blend, and hence may be neglected. The spectra of RR Tel and NGC 7662 are plotted in Figures 3 and 4, respectively, to illustrate the quality of the observational data, and to show the relative strengths of the O IV 1404.8 Å and S IV 1406.0 Å lines.

In Table 2 we summarise the electron densities derived from the observed values of R_1 – R_4 in conjunction with the calculations in Figures 1 and 2, along with the adopted electron temperatures from the references listed. An inspection of the table reveals that for NGC 3918 and NGC 7662 the derived densities are compatible, with values that differ by typically <0.2 dex from the mean estimates ($\overline{log\ N_e} = 3.7$ and 4.0 for NGC 3918 and NGC 7662, re-spectively). However in the case of V1016 Cyg, the electron density predicted from R_4 is approximately a factor of 50 lower than those estimated from R_1 and R_3. This is probably due to the fact that the 1397.2 Å line in the V1016

7

Cyg spectrum is weak and shows an asymmetry in the line profile, implying that it may be blended. We note that the observed R_4 ratio would need to be decreased by $\sim 20\%$ for it to give the same electron density as R_1 and R_3.

Also listed in Table 2 are the electron densities derived from line ratios in species with similar ionization potentials, and hence spatial distributions to O IV, such as $I(4711\ \text{Å})/I(4740\ \text{Å})$ in Ar IV. The values of $\log N_e$ estimated from $R_1 - R_4$ may be seen to be very similar to those deduced from other line ratios, with discrepancies that average only 0.2 dex, when the R_4 result for V1016 Cyg is excluded. In addition, we note that the observed ratios that are in the high density limit ($R_1 - R_4$ in RR Tel and R_2 in V1016 Cyg) only differ from the predicted high density values by $\leq 10\%$. These results provide experimental support for the accuracy of the present O IV line ratio calculations, and hence the atomic data employed in their derivation.

REFERENCES

Berrington, K.A., Burke, P.G., Butler, K., Seaton, M.J., Storey, P.J., Taylor, K.T., & Yu, Y. 1987, J. Phys. B, 20, 6379.

Blum, R.D., & Pradhan, A.K. 1992, ApJS, 80, 425.

Crees, M.A., Seaton, M.J., & Wilson, P.M.H. 1978, Computer Phys. Comm., 15, 23.

Dankworth, W., & Trefftz, E. 1977, J. Phys. B, 10, 2541.

Dufton, P.L. 1977, Computer Phys. Comm., 13, 25.

Dufton, P.L., Berrington, K.A., Burke, P.G., & Kingston, A.E. 1978, A&A, 62, 111.

Dufton, P.L., Hibbert, A., Kingston, A.E., & Doschek, G.A. 1982, ApJ, 257, 338.

Eissner, W., & Seaton, M.J. 1972, J. Phys. B, 5, 2187.

Fawcett, B.C. 1975, Atom. Data Nucl. Data Tables, 16, 135.

Feibelman, W.A. 1982, ApJ, 258, 548.

Flower, D.R., & Nussbaumer, H. 1975, A&A, 45, 145.

Hayes, M.A., & Nussbaumer, H. 1983, A&A, 124, 279.

————. 1986, A&A, 161, 287.

Kaler, J.B. 1986, ApJ, 308, 322.

Nussbaumer, H., & Storey, P.J. 1982, A&A, 115, 205.

Rowlands, N., Houck, J.R., Herter, T., Gull, G.E., & Skrutskie, M.F. 1989, ApJ, 341, 901.

Sandlin, G.D., Bartoe, J.-D.F., Brueckner, G.E., Tousey, R., & VanHoosier, M.E. 1986, ApJS, 61, 801.

Schmid, H.M., & Schild, H. 1990, MNRAS, 246, 84.

Seaton, M.J. 1964, MNRAS, 127, 191.

————. 1987, J. Phys. B, 20, 6363.

Stanghellini, L., & Kaler, J.B. 1989, ApJ, 343, 811.

FIGURE CAPTIONS

FIG. 1.–The theoretical O IV emission line ratio $R_1 = I(2s^22p\ ^2P_{3/2} - 2s2p^2$ $^4P_{1/2})/I(2s^22p\ ^2P_{3/2} - 2s2p^2\ ^4P_{5/2}) = I(1407.4\ Å)/I(1401.2\ Å)$, plotted as a function of logarithmic electron density (N_e in cm^{-3}) at electron temperatures of (from top to bottom), $T_e = 5000, 10000, 15000, 20000, 30000$ and 40000 K.

FIG. 2.–The theoretical O IV emission line ratio $R_2 = I(2s^22p\ ^2P_{3/2} - 2s2p^2$ $^4P_{3/2})/I(2s^22p\ ^2P_{3/2} - 2s2p^2\ ^4P_{5/2}) = I(1404.8\ Å)/I(1401.2\ Å)$, plotted as a function of logarithmic electron density (N_e in cm^{-3}) at electron temperatures of (from top to bottom), $T_e = 5000, 10000, 15000, 20000, 30000$ and 40000 K.

FIG. 3.–High resolution IUE spectrum (SWP 20247) of the symbiotic star RR Tel in the wavelength region 1396–1408 Å, where the flux is in units of ergcm^{-2}s^{-1}. The O IV lines at 1397.2, 1399.8, 1401.2, 1404.8 and 1407.4 Å are clearly labelled in the figure, as are Si IV 1402.8 Å and S IV 1406.0 Å. An emission feature due to a cosmic ray event is labelled in the figure with a cross.

FIG. 4.–High resolution IUE spectrum (SWP 4106) of the planetary nebula NGC 7662 in the wavelength region 1396–1408 Å, where the flux is in units of ergcm^{-2}s^{-1}. The O IV lines at 1397.2, 1399.8, 1401.2, 1404.8 and 1407.4 Å are clearly labelled in the figure, as are Si IV 1402.8 Å and S IV 1406.0 Å. An absorption feature due to a reseau mark is labelled in the figure with the letter R.
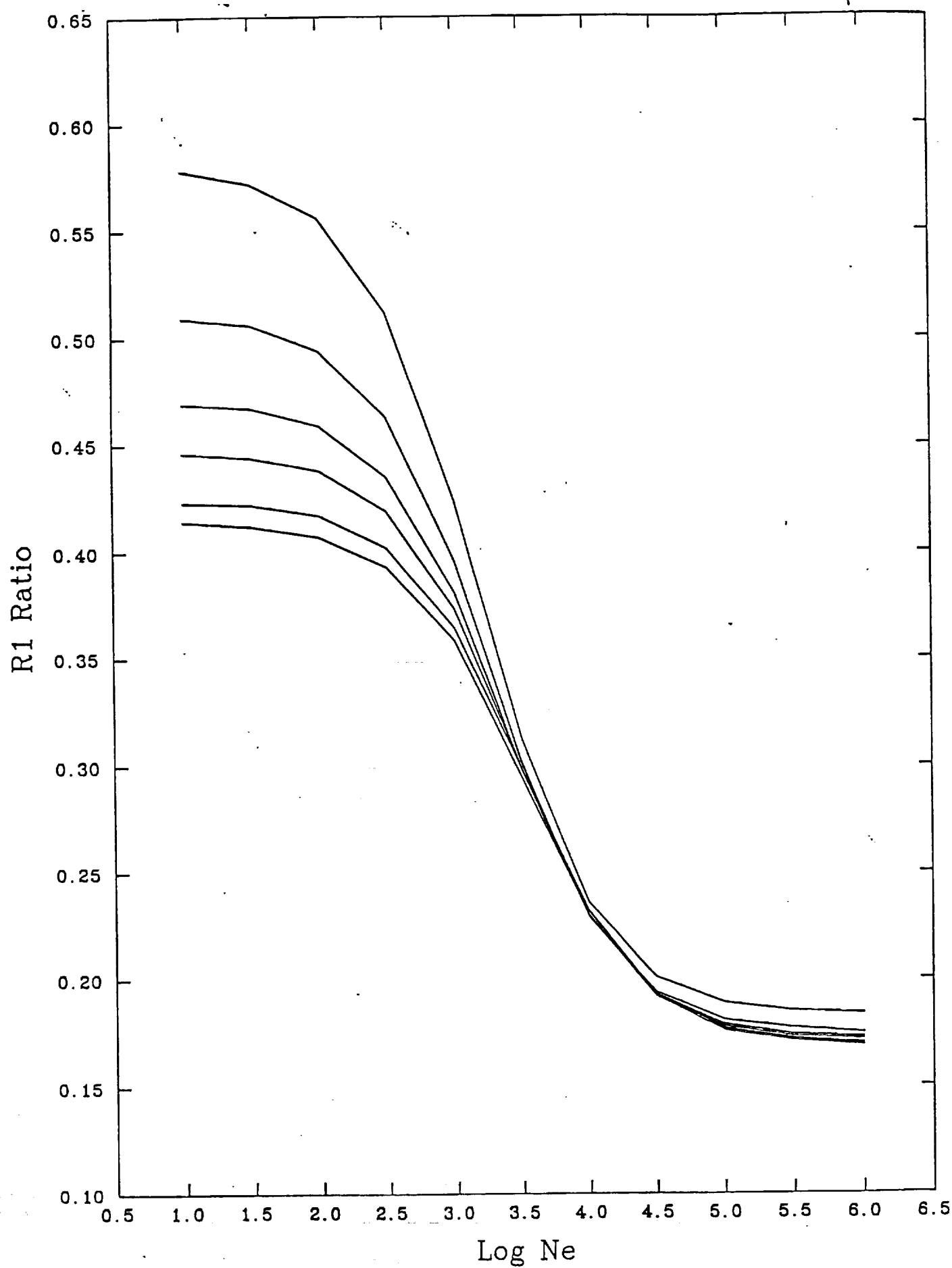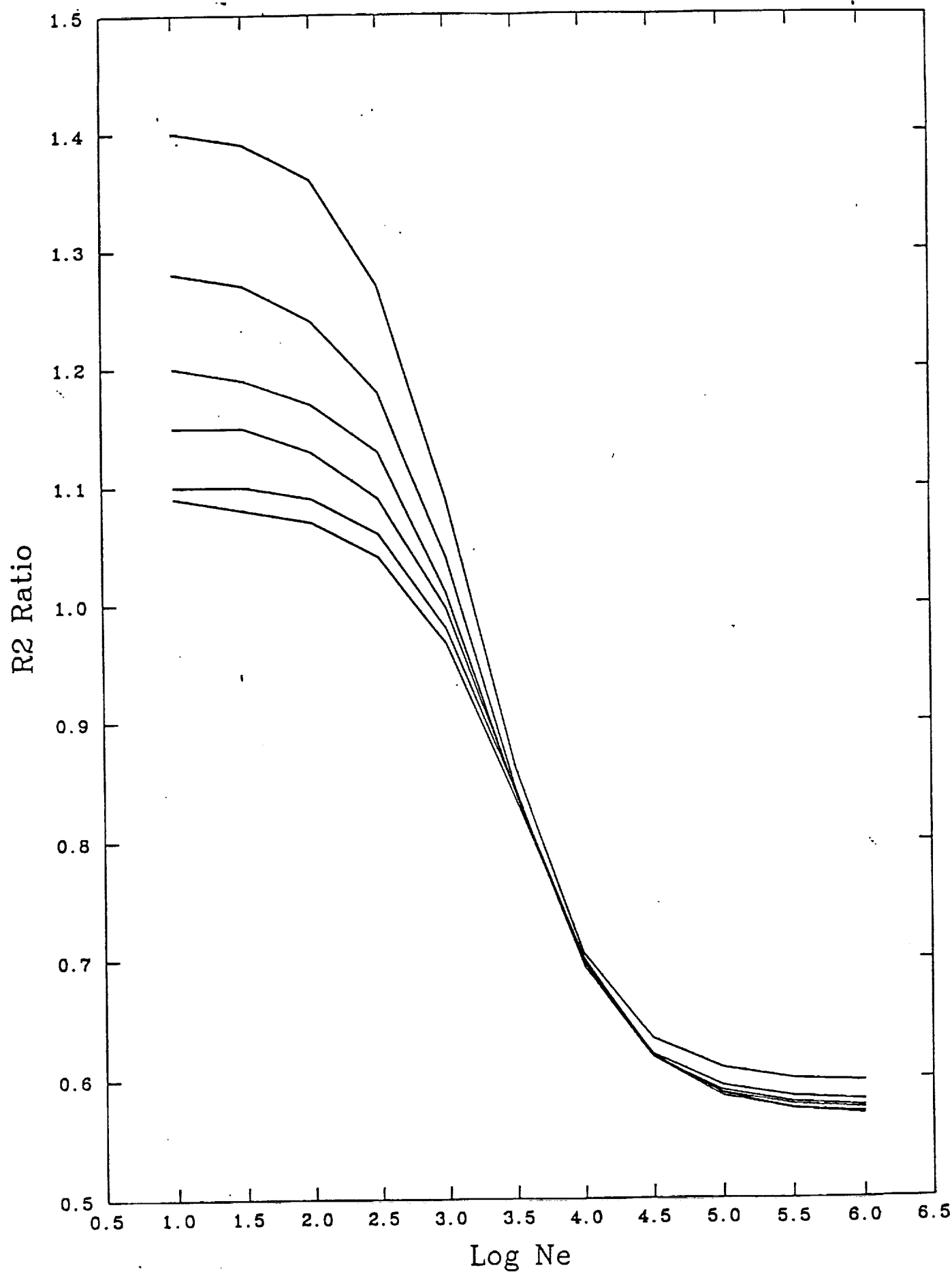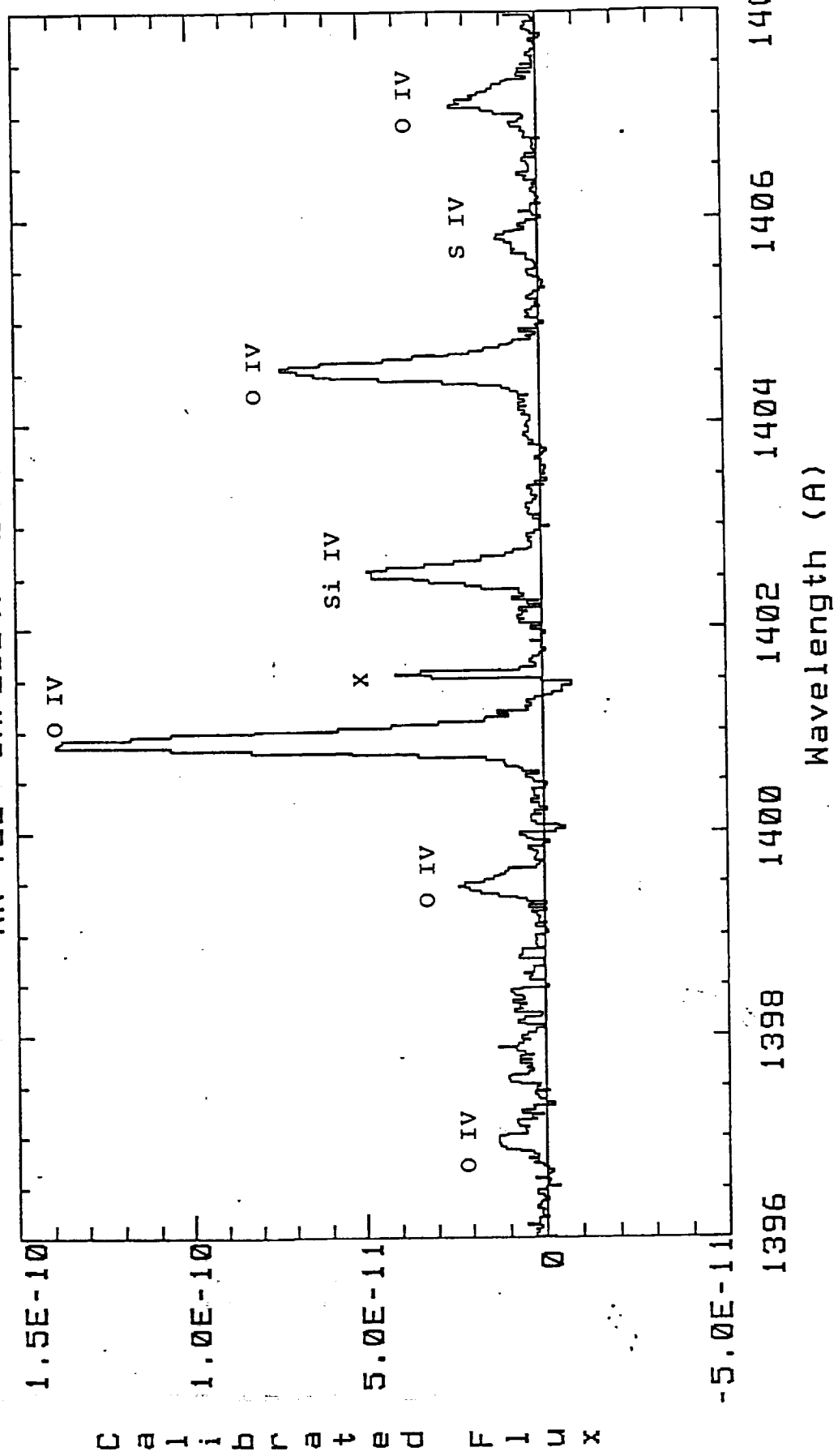
FIG 1

FIG 2

RR TEL SWP20247 20 min

FIG 3

NGC 7662 SWP04106H 408 min
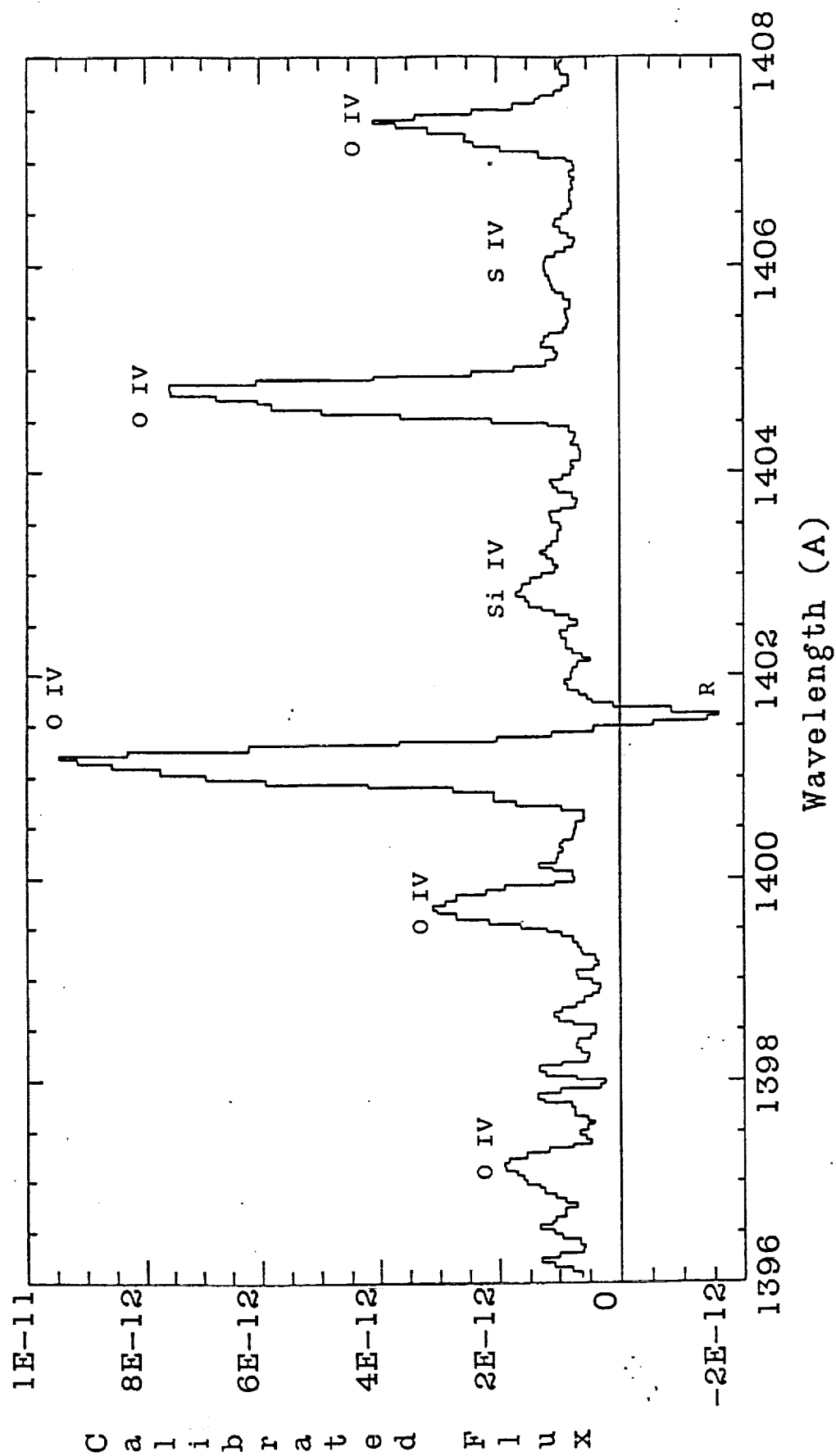
FIG 4

TABLE 1

OBSERVED O IV LINE INTENSITY RATIOS

Object	SWP Image Number	R_1	R_2	R_3	R_4
NGC 3918	19888	0.23	0.62	0.24	0.16
NGC 7662	4106	0.30	0.69	0.29	0.13
RR Tel	20247	0.15	0.55	0.14	0.10
V1016 Cyg	13432	0.17	0.51	0.19	0.12

TABLE 2

DERIVED O IV LOGARITHMIC ELECTRON DENSITIES

Object	T_e (K)	$\log N_e (R_1)$	$\log N_e (R_2)$	$\log N_e (R_3)$	$\log N_e (R_4)$	$\log N_e$ (other)
NGC 3918	14400[a]	3.6	3.9	3.6	3.8	3.5[b]
NGC 7662	12500[c]	4.0	4.3	4.0	3.5	3.8[b]
RR Tel	13000[d]	H[e]	H	H	H	6.4[d]
V1016 Cyg	30000[f]	5.8	H	5.6	4.0	5.9[f]

[a] Rowlands et al. 1989
[b] Stanghellini & Kaler 1989
[c] Kaler 1986
[d] Hayes & Nussbaumer 1986
[e] Indicates that the observed line ratio is smaller than the theoretical high density limit
[f] Schmid & Schild 1990

TABLE 2

DERIVED O IV LOGARITHMIC ELECTRON DENSITIES

Object	T_e (K)	$\log N_e$ (R$_1$)	$\log N_e$ (R$_2$)	$\log N_e$ (R$_3$)	$\log N_e$ (R$_4$)	$\log N_e$ (other)
NGC 3918	14400[a]	3.6	3.9	3.6	3.8	3.5[b]
NGC 7662	12500[c]	4.0	4.3	4.0	3.5	3.8[b]
RR Tel	13000[d]	H[e]	H	H	H	6.4[d]
V1016 Cyg	30000[f]	5.8	H	5.6	4.0	5.9[f]

[a] Rowlands et al. 1989
[b] Stanghellini & Kaler 1989
[c] Kaler 1986
[d] Hayes & Nussbaumer 1986
[e] Indicates that the observed line ratio is smaller than the theoretical high density limit
[f] Schmid & Schild 1990